Available online at www.sciencedirect.com
SCIENCE DIRECT®
Journal of Nuclear Materials 319 (2003) 87–94
journal of nuclear materials
www.elsevier.com/locate/jnucmat

Inert matrix fuel performance during the first two irradiation cycles in a test reactor: comparison with modelling results

Ch. Hellwig [a,*], U. Kasemeyer [b]

[a] Department of Nuclear Energy and Safety, Paul Scherrer Institut, CH-5232 Villigen PSI, Switzerland
[b] Nordostschweizerische Kraftwerke, Kernkraftwerk Beznau, Abt. Reaktor and Sicherheit, CH-5312 Döttingen, Switzerland

Abstract

In the inert matrix fuel (IMF) type investigated at Paul Scherrer Institut, plutonium is dissolved in the yttrium stabilised zirconium oxide (YSZ), a highly radiation resistant cubic phase with additions of erbium as burnable poison for reactivity control. A first irradiation experiment of YSZ based IMF is ongoing in the OECD Material Test Reactor in Halden together with mixed oxide fuel. The results of the first two cycles for IMF to a burnup of some 105 kW d cm^{-3} are presented and the modelling results in comparison with the experimental results are shown. A first approximation for a simple swelling model for this YSZ based IMF can be given. Possible fission gas release mechanisms are briefly discussed. The implications of the modelling results are discussed.

PACS: 28.41.Ak; 28.41.Bm

1. Introduction

In inert matrix fuel (IMF), plutonium is embedded in an U-free matrix. This allows plutonium to burn without breeding any new plutonium by neutron capture in ^{238}U and therefore a more efficient consumption of plutonium is achieved compared to mixed oxide fuel (MOX). The fuel research at Paul Scherrer Institut (PSI) concentrated the latest efforts in this field on a zirconia based matrix. In this fuel, plutonium is dissolved in the yttria stabilised zirconia (YSZ), a highly radiation resistant cubic phase with the potential of achieving a high burnup [1]. The chemical stability of the chosen matrix leads to further advantages as preventing the wash-out of fissile and fission products in case of cladding failure in the reactor, having the fission products already embedded in an inert matrix for final disposal [2], and increased proliferation resistance. IMF is designed to be used similar to MOX in conventional fuel assemblies. Erbium as burnable poison has to be added to IMF to lower the high reactivity at begin of life [3].

This new fuel candidate was well investigated [4–9], before first irradiation experiments of YSZ based IMF were started. One of these irradiation experiments is ongoing in the OECD Material Test Reactor in Halden together with MOX fuel (Rig IFA-651.1) [10]. The results of the first cycle of the experiment and the connected modelling are presented in [11]. Table 1 gives an overview of the IMF rods in this experiment.

For modelling, calculations with a modified version of the TRANSURANUS (V1M2J00) code [12,13] were performed. Different material correlations and models dedicated to YSZ based IMF were implemented in the TRANSURANUS-IMF version. For the calculation of the first two cycles, several models and correlations were updated.

* Corresponding author. Tel.: +41-56 310 2666; fax: +41-56 310 2203.
E-mail address: christian.hellwig@psi.ch (Ch. Hellwig).

0022-3115/03/$ - see front matter
doi:10.1016/S0022-3115(03)00138-7

Table 1
Instrumentation and characterisation of the IMF rods in IFA-651.1

Rod no.	2	4	5
Fuel designation	IMF-ATT	IMF-CO	IMF-ATT
Fabrication method	Dry mill	Co-precipitation	Dry mill
Instrumentation[a]	TF, PF, EF	TF, PF, EF	ET, PF
Fuel density (% TD)	95.2	85.6–92.0	95.3
Grain size[b] (μm)	2	20	2
Fuel stack length (mm)	477.4	479.9	497.8
Rod free volume (%)	30	30	30

[a] ET: expansion thermometer; TF: thermocouple; PF: pressure transducer; EF: stack elongation detector.
[b] Approximation only.

The present report gives an overview of the IMF-related improvements of the TRANSURANUS code, shows modelling results of the first two cycles for all three IMF rods in IFA-651.1 and discusses the crucial parameters responsible for fission gas release (FGR) in this experiment.

2. Modification of material correlations and models

Recently, the thermal conductivity model was updated according to out-of-pile measurements of fuel samples in the Pu-laboratories of ITU, Karlsruhe up to temperatures of 1902 K. The thermal conductivity κ [$\mathrm{W\,m^{-1}\,K^{-1}}$] derived from these measurements is described by the correlation:

$$\kappa = \frac{1}{0.403 + 0.00013 \cdot T} + 1.1 \times 10^{-11} \cdot T^3, \tag{1}$$

where κ is the thermal conductivity of IMF with 95% of theoretical density, and T is the temperature.

Thus the thermal conductivity of fresh IMF shows a slight dependence on temperature and is low compared to MOX fuel. In this investigation, no burnup dependence is taken into account for the thermal conductivity of IMF as it is supposed to be negligible due to the already strongly distorted lattice in non-irradiated YSZ [14]. With the first two cycles of IFA-651.1, an average IMF burnup of 105 $\mathrm{kW\,d\,cm^{-3}}$ is reached. This burnup corresponds to about 10.5 $\mathrm{MW\,d\,kg^{-1}}$ for MOX that shows already at this burnup a significant decrease in thermal conductivity, according to commonly used correlations.

In the course of the present investigation, the swelling strain had to be adjusted to fit the calculation to the experimental fuel elongation data. The swelling strain was set to 0.1% per % FIMA for the open gap condition. (The value for UO_2 is roughly 10 times higher.) It must be mentioned, that from two IMF fuel elongation measurements, one got blocked during the second cycle before the densification came to an end. Therefore this new swelling strain correlation depends more or less on only one measurement and must be regarded as approximation only.

The densification is burnup dependent only and is treated according to the empirical TRANSURANUS correlation:

$$\eta(\mathrm{bu}) = \eta_\infty + (\eta_0 - \eta_\infty) \cdot \exp\left(-\frac{5}{\mathrm{bu}_0} \cdot \mathrm{bu}\right), \tag{2}$$

where $\eta(\mathrm{bu})$ is the sinter porosity, η_∞ is the porosity at end of densification (given in input), η_0 is the fabrication porosity (given in input), bu is the average burnup in the axial fuel element, and bu_0 is a burnup constant (given in input).

The resulting loss of pellet volume is divided into an axial part (affecting the fuel elongation) and a planar part. The planar part is divided into an increase in the pellet inner crack volume and – to a lesser extent – to the decrease of the pellet outer diameter.

The pore migration model and the grain growth model were left unmodified with the original data of UO_2. As the evaporation–condensation effects for the pore migration model as well as the self-diffusion coefficient responsible for the grain growth are weakly connected with the melting temperatures (T_M) of the material, this is regarded as a valid first approximation (T_M for UO_2 is 3113 K, T_M for YSZ is around 2990 K, depending on the yttria concentration).

The standard TRANSURANUS FGR model was chosen as the base for the IMF FGR model. In this standard model, an effective thermal diffusion coefficients is used:

$$D_\mathrm{eff} = 5 \times 10^{-8} \cdot \mathrm{e}^{-40\,262/T}, \tag{3}$$

where D_eff [$\mathrm{m^2\,s^{-1}}$] is the effective thermal diffusion coefficient.

The lowest possible value for the diffusion coefficient is that of the athermal diffusion coefficient, therefore

$$D_\mathrm{eff} \geqslant 10^{-25}. \tag{4}$$

The model includes also a simple grain boundary model where a certain amount of fission gas can be found on the grain boundaries. Fission gas exceeding the maximal grain boundary concentration is assumed to be immediately released to the plenum.

3. Fuel behaviour

The fuel behaviour of IFA-651.1 rods during the first two cycles can be summarized as follows: The measured center temperatures for the fresh fuel were within the expected range for both, IMF and MOX fuel. All IMF rods reached significantly higher temperatures due to the lower thermal conductivity compared to MOX. The pressure was decreasing during the first cycle in all six rods due to fuel densification, the fuel densification being more distinct in IMF than in MOX. MOX fuel showed no significant FGR. FGR in IMF was not detected before the ramp phase in the second cycle, where the local heat rates increased temporarily to 40 $kW\,m^{-1}$ in maximum.

The fuel densification could also be observed by stack elongation measurements and ended after about 65 $kW\,d\,cm^{-3}$ in case of the dry-milled IMF (IMF-ATT, i.e. fabricated by a dry attrition milling procedure at PSI) and is still ongoing for the co-precipitated IMF (IMF-CO, powder fabricated by internal gelation at PSI with subsequent crushing of the calcined spheres). The densification of the MOX fuel was found to be reasonably low (1–2%). The densification in IMF was unexpectedly high and led to nearly 100% dense fuel in case of the IMF produced by attrition milling. In spite of the strong densification, the fuel temperatures of IMF stayed rather stable.

4. Fuel modelling

4.1. Fuel temperatures

Rod 2 contained IMF-ATT and was equipped with a fuel thermocouple (TC), a pressure transducer and a stack elongation sensor. The TC was inserted some 84 mm in annular pellets of 98.4 mm stack length, while the whole stack length, annular and solid pellets, was 477.4 mm. For modelling, the rod was divided into 10 axial slices of equal length. The tip of the thermocouple was assumed in the center of the ninth slice. The useful temperature results of rod 2 are restricted to the first cycle, as later the thermocouple showed some malfunctioning. The temperature calculated for the TC position is close to the measured temperature (70 K maximum difference). The calculated temperature of the hottest pellet (solid, not annular) at the maximum local power of 40.0 $kW\,m^{-1}$ was calculated to 2314 K.

The temperature in rod 5 (contains also IMF-ATT) is measured with an extension thermometer, i.e. the measured temperature reflects an average fuel center temperature over the whole fuel stack of annular pellets. Measurement and calculation are in good agreement, see Fig. 1. This is especially true for the four ramps plotted in detail in Fig. 2. The four chosen ramps are evenly distributed over the burnup. Obviously, a burnup correction of the thermal conductivity is not necessary for the investigated burnup range.

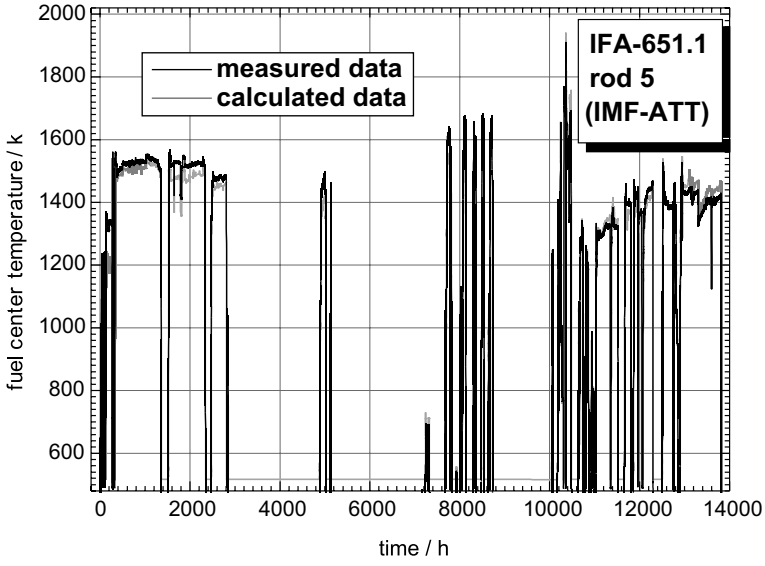

Fig. 1. Calculated and measured fuel center temperature versus time for IFA-651.1, rod 5 (IMF-ATT).

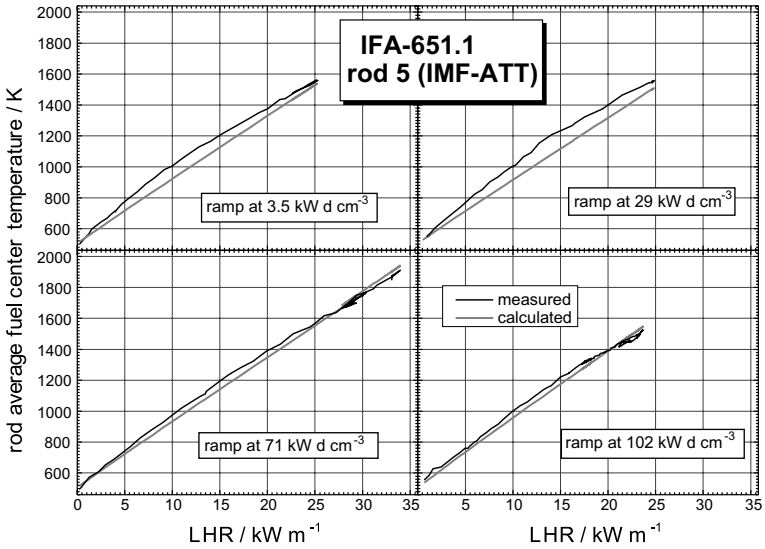

Fig. 2. Calculated and measured fuel center temperature for four ramps, rod 5 (IMF-ATT).

While rods 2 and 5 consist of IMF-ATT, rod 4 consists of IMF-CO. The main differences are the much larger grain size and the higher as-fabricated porosity in IMF-CO. The TC position in rod 4 was comparable to rod 2. Fuel behaviour calculations were performed with the same thermal conductivity correlation and the same relocation model as for the former two rods. Figs. 3 and 4 show a similarly good agreement between measured and calculated temperatures. The calculated temperature of the hottest pellet (solid, not annular) reaches 2272 K at the maximum power of 35.6 kW m^{-1} due to its higher porosity compared to IMF-ATT.

4.2. Fuel elongation

The fuel elongation measurements deliver information about the densification and the swelling. Two elongation sensors have been inserted in IMF rods, one in rod 2 (IMF-ATT) and one in rod 4 (IMF-CO). Fig. 5 shows the fuel elongation of rod 2 versus rod average

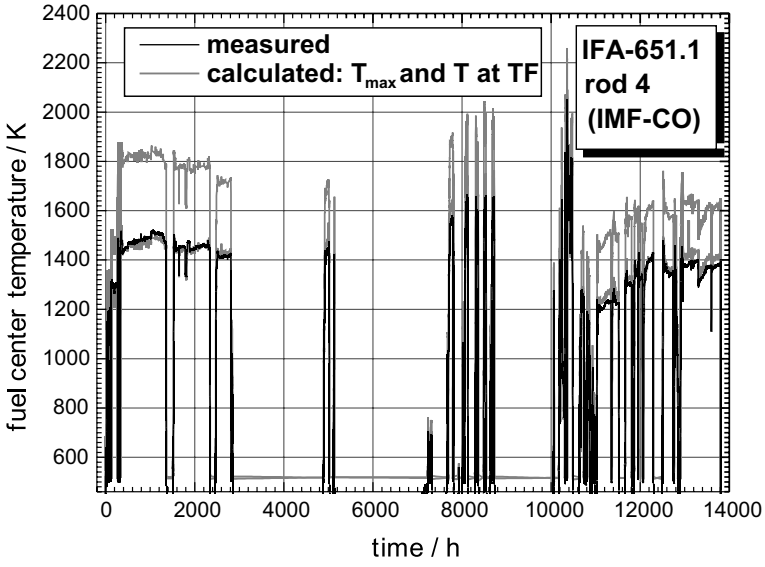

Fig. 3. Calculated and measured fuel center temperature versus time for IFA-651.1, rod 4 (IMF-CO).

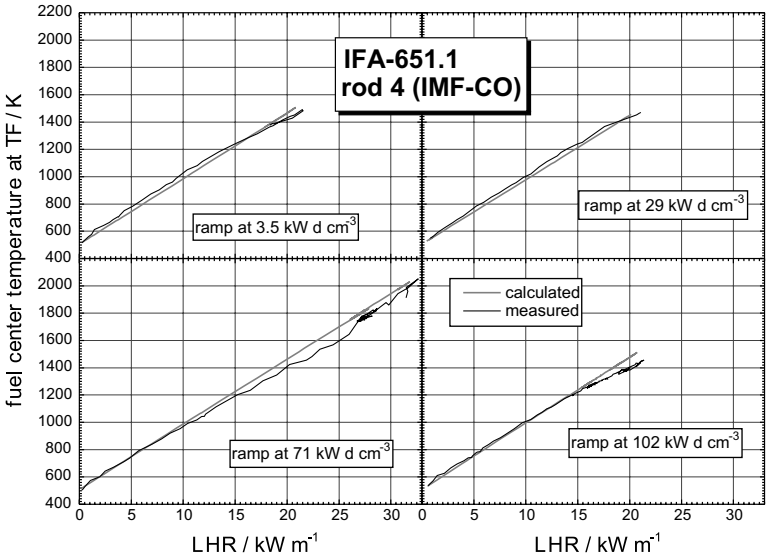

Fig. 4. Calculated and measured fuel center temperature at the thermocouple for four ramps, rod 4 (IMF-CO).

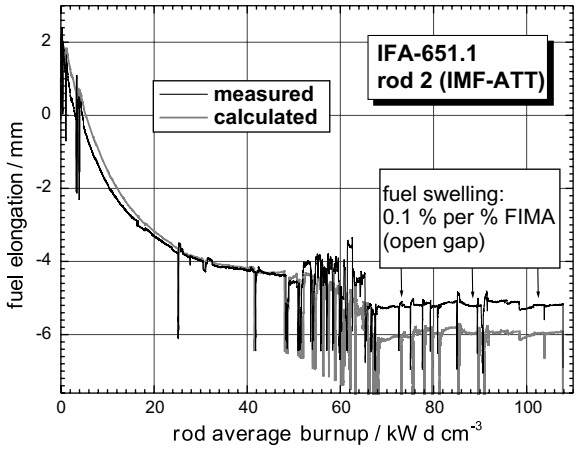

Fig. 5. Measured and calculated fuel stack elongation for IFA-651.1, rod 2. After the sintering has come to an end, the fuel swelling rate could be estimated.

burnup. The pronounced densification ends up with nearly 100% dense material (this is not extraordinary, as YSZ is known to have a very good sinter ability) after a burnup of some 65 kW d cm^{-3}. The densification is probably also accelerated by the small initial grain size. After the densification has come to an end, the fuel swelling can be determined to around 0.1% per % FIMA for the observed burnup range, i.e. a tenth of the normal UO_2 swelling rate. With this swelling correlation, the measured and the calculated fuel elongation curves in Fig. 5 are in parallel. It must be mentioned that this simple correlation does not distinguish between solid and gaseous swelling and does not allow extrapolation to high burnup with possibly increased gaseous swelling. The calculated data show a decrease of the fuel stack length during the ramp phase due to fuel creep. This decrease cannot be observed in the experiment. As the used creep correlation in TRANSURANUS-IMF is the UO_2-standard correlation, the creep resistance of the investigated type of IMF seems to be significantly higher than that of UO_2. The creep resistance model was not adjusted until now, because the relative complicate model would require more data for a reasonable adjustment. Additionally, there is no necessity for this as the calculated difference in stack elongation has no significant effect on other important parameters.

The fuel elongation measurement of rod 4 with IMF-CO revealed a slower densification. The large grains of the material fabricated by internal gelation might slow down the process. At the same time, the higher initial porosity (average pore size of roughly 3.5 μm) and the excellent sinter ability of YSZ allows a stronger densification. Therefore the densification has not ended until the end of the second cycle.

4.3. Fission gas release

FGR can be monitored by the pressure transducers, of which one is present in every rod. While FGR increases the rod inner pressure, densification decreases it. Therefore the initial densification must be modelled accurately enough to be able to separate the pressure effect by FGR. Fortunately, this is possible by using the data of the early period under 10 kW d cm^{-3}, were no FGR can be observed, and by the fuel elongation measurements.

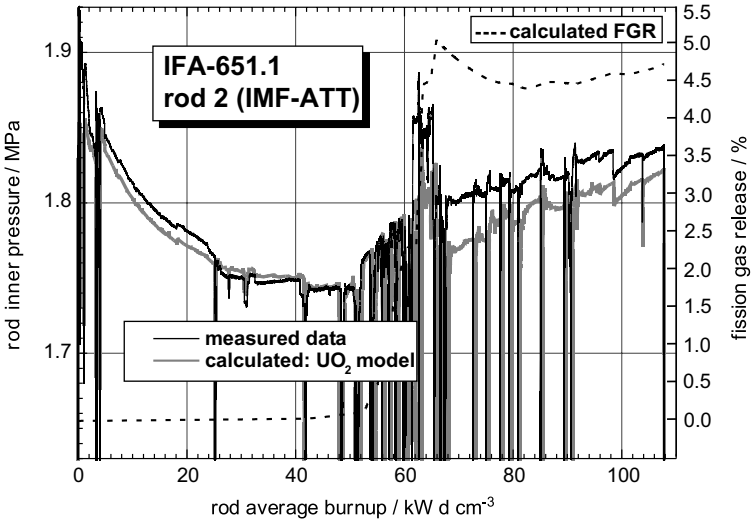

Fig. 6. Measured and calculated pin inner pressure for IFA-651.1, rod 2. The right axis corresponds to the plotted calculated fission gas release. The pressure decrease is caused by the increase of open volume due to fuel densification, the increase by fission gas release (FGR). FGR was calculated using a maximal concentration of fission gas on the grain boundaries of 0.00012 μmol mm^{-3}.

Fig. 6 shows the measured rod inner pressure of rod 2 (IMF-ATT) versus rod average burnup. Additionally, the calculated values using an UO_2 FGR model are plotted as well as the calculated FGR. The agreement between measurement and calculation is acceptable although the FGR-peak during the short high-power period at about 60 kW d cm^{-3} cannot be completely simulated by calculation. It must be mentioned, that this agrees well with our experience with this particular FGR model: FGR during short high-power periods is normally underestimated for UO_2 and MOX.

In the present calculation, the grain growth (calculated with an UO_2-model) is responsible for the major amount of the FGR. During grain growth, grain boundaries move through the fuel and accumulate fission gas. Fission gas is literally 'swept out' by the grain boundary movement. For IMF-ATT with the small initial grain size, a distinct grain coarsening is modelled during the irradiation. Therefore the pure diffusion equation for the diffusion of fission gas atoms to the grain boundaries plays a negligible role in the present case and no statements can be given about its validity for IMF. It has to be emphasized that the whole interpretation depends on calculations based on UO_2-correlations. In case of rod 2 the calculated results are in good agreement with the measured data, but this is by no means a validation of the applicability of the UO_2 grain growth model to IMF. Reliable experimental data about the grain size, as-fabricated and after irradiation, remains crucial.

The rod inner pressure for rod 5 (IMF-ATT) showed a higher FGR than calculated with the above used model (the calculation would give 0.1% FGR, compared with 7.5% FGR estimated by measured rod inner pressure). A good agreement with the measured data could be reached by lowering the maximal FG concentration on the grain boundaries to a sixth of the original value. This facilitates the FGR from the grain boundaries and leads to higher FGR. A certain physical meaning might be derived from the fact that all pellets are annular pellets in this rod and the larger inner surface could contribute to the release, especially during grain growth. But it remains an open question, if this adjustment was justified, until PIE results confirm or contradict this simple approach.

Fig. 7 shows the measured and calculated rod inner pressure as well as the calculated FGR for rod 4 (IMF-CO). IMF-CO has larger grains and higher initial porosity. The same FGR model as for rod 5 (i.e. the UO_2-model with reduced maximal fission gas concentration on the grain boundaries) fails to model the distinct FGR during and after the high-temperature phase. A modification of the FGR model parameter within a reasonable range did also not lead to a satisfying simulation of this distinct FGR. Due to the larger initial grain size, no significant grain growth was calculated for this rod with the UO_2 grain growth model. Various mechanisms might be responsible for this misfit between experimental and calculated results: (i) the grains are still growing, sweeping out fission gas, although no grain growth would be anticipated for UO_2, (ii) fission gas might be swept to the grain boundaries by pore migration, although only very little pore migration is calculated with the UO_2-model, and (iii) a combination of these effects.

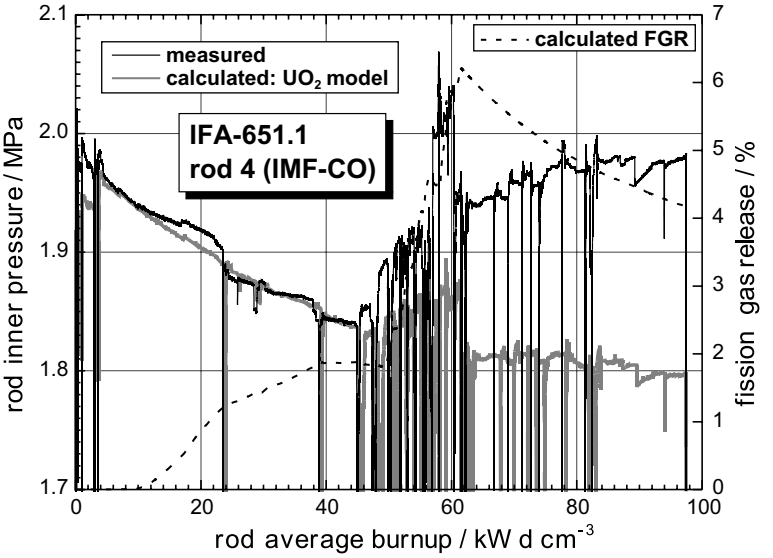

Fig. 7. Measured and calculated pin inner pressure for IFA-651.1, rod 4. The right axis corresponds to the plotted calculated fission gas release. The pressure decrease is caused by the increase of open volume due to fuel densification, the increase by fission gas release (FGR). FGR was calculated using a maximal concentration of fission gas on the grain boundaries of 0.00002 μmol mm^{-3}.

It might also be necessary to adjust the diffusion equation, but as the variation of the diffusion coefficient and activation energy could not reproduce the experimental results qualitatively, this must wait until the experimental results can be met at least qualitatively.

5. Conclusion and outlook

The IMF/MOX irradiation test in Halden delivered a large amount of valuable data until now, although for the IMF rods, a thermocouple and an elongation sensor failed recently. The TRANSURANUS code with the modifications described in this report and earlier was used to model the IMF rods during the first two cycles of the experiment, although the FGR modelling including grain growth and pore migration was performed with UO_2 data as IMF data are not available for these phenomena. The value of these calculations is to indicate which the crucial parameters are to be investigated experimentally.

In general, the following can be concluded:

- Fuel temperatures can be modelled well with the new correlation for thermal conductivity without any burnup-dependence (up to some 103 kW d cm^{-3}). Good agreement was achieved in IFA-651.1 until nearly 2073 K. The relocation was set to half of that of UO_2 to adjust the calculated to the measured fuel center temperatures.
- Fuel elongation can be modelled well with the proposed densification model and a swelling rate of 0.1% per % FIMA for open gap conditions (compared to some 1.0% per % FIMA for UO_2).
- The observed FGR kinetic during and after the high-temperature phase indicates that FGR in the investigated rods might be highly affected by grain growth and pore migration and less by gas diffusion to the grain boundaries. Therefore the adjustment of the diffusion data from UO_2 to IMF is impossible now.
- Reliable data on grain size and pore distribution from PIE is of first priority to model FGR more reliable.

The experiment will be further continued until 2005. Certain efforts will be undertaken to repair the malfunctioning sensors. The removal of one fuel rod for early PIE during the next year is discussed as the possible fuel restructuring would deliver important results for the interpretation of the IMF behaviour and for a possible, improved fuel fabrication. An improved fuel fabrication should – based on the current interpretation – aim at larger grains and less porosity to restrict the FGR as well as the densification.

Acknowledgements

The contributions of G. Ledergerber and C. Degueldre to the IMF research at PSI are gratefully acknowledged. The fabrication and irradiation became possible by the collaboration with KAERI (D.S. Sohn, Y.-W. Lee, H.S. Kim), BNFL (Ch. Brown, G.A. Gates) and the OECD Halden Project (G. Rossiter, B.H. Lee

and T. Sugiyama). The fuel fabrication was performed by P. Heimgartner, R. Zubler, F. Ingold, and J. Wichser. The work at PSI was financially supported by the Swiss utilities.

References

[1] C. Degueldre, U. Kasemeyer, F. Botta, G. Ledergerber, Mater. Res. Soc. Symp. Proc. 412 (1995) 15.
[2] E. Curti, W. Hummel, J. Nucl. Mater. 274 (1999) 189.
[3] U. Kasemeyer, R. Chawla, P. Grimm, J.M. Paratte, Nucl. Technol. 122 (1998) 52.
[4] U. Kasemeyer, Konzeption eines uranfreien LWR-Kerns zur Plutoniumverbrennung, thesis, EPFL Lausanne (CH), 1998.
[5] M.A. Pouchon, Contribution to the study of a zirconia based nuclear fuel for plutonium use in light water reactor, thesis, Universität Genf (CH), 1999.
[6] Y.-W. Lee, H.S. Kim, S.H. Kim, C.Y. Joung, S.C. Lee, S.H. Na, P. Heimgartner, G. Ledergerber, Prog. Nucl. Energy 38 (2001) 231.
[7] M. Burghartz, G. Ledergerber, F. Ingold, P. Heimgartner, C. Degueldre, Prog. Nucl. Energy 38 (2001) 247.
[8] C. Degueldre, M.A. Pouchon, M. Streit, O. Zaharko, Prog. Nucl. Energy 38 (2001) 241.
[9] M.A. Pouchon, C. Degueldre, M. Döbeli, Prog. Nucl. Energy 38 (2001) 275.
[10] U. Kasemeyer, Ch. Hellwig, Y.-W. Lee, G. Ledergerber, D.S. Sohn, G.A. Gates, W. Wiesenack, Prog. Nucl. Energy 38 (2001) 309.
[11] Ch. Hellwig, U. Kasemeyer, G. Ledergerber, B.-H. Lee, Y.-W. Lee, R. Chawla, Ann. Nucl. Energy 30 (2003) 287.
[12] K. Lassmann, J. Nucl. Mater. 188 (1992) 295.
[13] K. Lassmann, A. Schubert, J. van de Laar, C.W.H.M. Vennix, in: IAEA Technical Committee Meeting on Nuclear Fuel Behaviour Modelling at High Burnup, Lake Windermere, UK, June 2000.
[14] C. Degueldre, T. Arima, Y.W. Lee, J. Nucl. Mater., these Proceedings.